

INTENSE LOW EMITTANCE LINAC BEAMS FOR FREE ELECTRON LASERS*

T. I. Smith

High Energy Physics Laboratory
Stanford University
Stanford, California 94305-4080

Abstract

New approaches to linear accelerator design are necessary in order to produce the intense low emittance beams required for Free Electron Laser operation. Examples are the use of high gradient single cell or dual cell resonators instead of conventional multi-cavity structures, the use of multiple frequency (harmonically related) rf fields for acceleration instead of single frequency fields, and the use of magnetic bunching at relatively high energies instead of conventional bunching at low energy. Advantages of the use of multiple frequency rf fields will be discussed, and the results of numerical calculations comparing multiple frequency vs. single frequency acceleration will be presented.

Introduction

The parameters of an electron beam intended for use in a Free Electron Laser (FEL) are subject to several constraints. The most obvious is that placed on the beam energy by the FEL resonance condition¹ which relates the energy, the optical wavelength, the wiggler wavelength, and the wiggler magnetic field. Another constraint appears as a result of the requirement of spatial overlap of the optical beam and the electron beam through the interaction region. Under some modest simplifying assumptions, primarily that there is no focussing of the electron beam along the interaction region, this constraint reduces to the requirement that the absolute emittance of the electron beam be no larger than the optical wavelength. (In applying this restriction, the emittance is understood to be the area of the x vs. dx/dz or y vs. dy/dz phase space measured in length-radians.) The final constraint to be considered is a limit to the energy spread which can be tolerated on the beam. In order for the electron and optical beams to interact coherently over the length of the wiggler, the fractional energy spread of the beam cannot be larger than about $1/2N$, where N is the number of periods in the wiggler. Finally, since the gain of the system is directly proportional to the peak current of the electron beam, it is desirable that the peak current be as large as possible. Linac based FELs can operate with peak currents of only a few amperes, but values of 100 amperes are more desirable and interesting.

These constraints can best be understood in the context of a specific example. Assume that a 2000 Å FEL is desired, and that it is to be powered by a 150 MeV electron beam. The 'resonance' condition immediately sets a wiggler wavelength of 1.8 cm, if the wiggler field is chosen to be a reasonable value. An acceptable choice for the length of the wiggler is 3 meters ($N=167$). With this length the small signal gain for the FEL is calculated to be 2% Amp and the upper limit on the energy spread is 0.3%. Assuming a bunch length of 1/100 of an rf cycle (3.6 deg) and a charge per bunch of 1 nC, the peak current will be 100 Amperes (for a gain per pass of 200%), while the longitudinal emittance of the beam must be less than 520π KeV deg. The requirement that the transverse emittance (ϵ_t) be no larger than the optical wavelength sets an upper

limit on ϵ_t of .2 mm mr, or $.06 \pi$ mm mr. In terms of the relativistically invariant 'normalized' emittance ($\epsilon_n = \beta \gamma \epsilon_t$, $\epsilon_n \leq 19 \pi$ mm mr.

The normalized emittance from a 1 cm^2 thermionic cathode delivering a continuous beam of 1 Ampere is 8π mm mr.² If all of the charge in one rf cycle were to be bunched to 3.6° , the peak current from such a cathode should be approximately 100 Amperes. While it is admittedly unrealistic to expect to bunch all of the current in one cycle, it is also true that substantially more than one Ampere can be expected from the assumed cathode. If the beam from a thermionic cathode were accelerated in an rf linac without any degradation in phase space, peak currents on the order of 100 Amperes and normalized transverse emittance on the order of 10π mm mr would be available. Data for the various linac based FEL projects underway in the world at this time are presented in Table 1. From the table it is apparent that none of the linacs deliver a beam with both the high peak current and the low emittance. The first three projects listed make use of existing linac technology, adapting it to FEL use through the installation of subharmonic bunchers and additional diagnostics in the injector. Although this approach has been fruitful, particularly for the Boeing project, further progress will be extremely difficult without utilizing new approaches to linac design. Indeed, the fourth project listed, the MK III IRFEL project, makes use of an innovative rf gun designed explicitly to provide pulsed intense low emittance beams for FEL operation. The last project listed, the SCA/TRW collaboration, makes use of the Stanford Superconducting Accelerator which was designed to produce a very precise low current beam for nuclear physics purposes. The emittance produced is very small, but so is the peak current.

TABLE 1

Linac Based FEL Projects

	operating* wavelength (microns)	normalized emittance (π mm mr)	peak current (Amperes)
LANL	10	120	100
Boeing	(.5)	30	100
UK FEL	(10)	50	5-10
MK III FEL	3	10	20
SCA/TRW	1.6(.5)	5	2-4

* Values in parenthesis indicate wavelength goals.

Beam brightness, (defined as $2 \pi^2 i_{\text{peak}} / \epsilon_n^2$) is frequently used as a measure of beam quality for FELs, even though it does not address the fact that high current and small emittances are necessary simultaneously. Much of the present enthusiasm for the use of the electron beam circulating within a storage ring to power an FEL stems from the high brightness and large peak currents of such a beam. It is interesting to note that the brightness and peak current of the bunched beam from a good gun are at least as good as those of storage rings. Thus a successful program of preserving the quality of the beam produced by the gun throughout

* This work was supported by ONR Contract No. N00014-85-K-0348.

the acceleration process would allow a linac beam to power the same sorts of FELs as storage rings, but without some of the power and efficiency limitations.

Phase Space Dilution

The various mechanisms responsible for the phase space dilution of the beam as it progresses along the linac can be conveniently placed into four classes: transport aberrations, beam induced field effects, space charge effects, and rf dynamics effects. Of the three classes, transport aberrations are at present the least serious -- they are well understood and careful attention to detail can reduce their effects to acceptable levels. Space charge, rf dynamics effects, and beam induced field effects are more troublesome, and need to be considered further.

Beam induced field effects which cause phase space dilution include various beam breakup interactions, and various single and multi-bunch wake field effects. The control of these effects is a particularly severe problem in conventional linear accelerators which have traditionally been designed to use rather long microwave structures consisting of many coupled rf cavities of high shunt impedance. The advantages of these conventional structures are that they couple cavity fields rather efficiently to the beam, and their geometry maintains a coherent accelerating field over their entire length with only a single rf driving source. For high brightness linacs these advantages can be liabilities: the beam can drive cavity fields easily and the driven fields have the entire length of the structure in which to interact with the beam. Our group at the High Energy Physics Laboratory at Stanford University has been studying the advantages of using high gradient single or dual cell resonators to produce high brightness beams. The simplicity of these resonators provides several benefits: their mode structure can be accurately calculated by computer codes such as URMEI;³ their higher order modes can be relatively easily loaded; their short length automatically reduces the strength of some types of beam-cavity interactions. Further benefits arise if the cavities are superconducting. The high cw field gradients achievable in superconducting cavities reduce the phase space dilution due to beam induced fields by allowing a reduction of the accelerator's length. In addition, rf losses in superconducting cavities are low enough that cavity geometries can be chosen to minimize induced field problems, rather than to maximize shunt impedance. For a more complete discussion the reader is referred to reference 4.

Space charge effects are in a real sense fundamentally unavoidable. If a beam is cylindrically symmetric, uniformly charged, hard-edged, and has no ends, then the space charge forces act as an ideal lens and cause no growth in the occupied phase space. As real beams generally satisfy none of these requirements, space charge forces will enlarge the phase space, and the best that can be done is to reduce the magnitude of the forces as much as possible. One obvious method of reducing the magnitude of the forces for a bunch of constant charge is to increase its dimensions. This clearly implies low frequency operation, since the allowable beam dimensions will scale much like the operating wavelength. (Precise scaling statements require knowledge of the rf field scaling.) Another method for reducing the importance of the space charge forces is to accelerate the charge bunch as rapidly as possible, in order to take advantage of relativistic effects. This argues in favor of high field gradients in the rf accelerating cells and in the electron gun. In addition,

relativistic effects suggest that if the linac contains a dc injector section, then the beam voltage in this section should be as high as reasonable. Finally, since it is certain that the ends of the beam will be affected differently by space charge forces than the center, it is important to keep the bunch as long as possible and to choose the beam diameter which is the best compromise between the reduced end effect associated with a small diameter and the decreased space charge forces associated with a large diameter.

Phase space dilution due to rf phase effects occurs because different electrons experience different rf phases as they pass through a cavity. Thus they gain different amounts of energy and experience different transverse forces. For relativistic electrons interacting with a sinusoidally time varying field the energy gain of an electron is proportional to the cosine of the phase angle between its position and the position of maximum energy gain. A mono-energetic electron beam of finite length (zero longitudinal phase space) entering such an accelerating field will leave with a spread in energy and a finite longitudinal phase space. Consideration of the transverse forces leads to a similar conclusion with regard to transverse phase space. In a cylindrically symmetric, sinusoidally time varying field an electron will experience a radial focussing force which is proportional to the sine of its phase angle (defined above). Thus electrons in front of the position of maximum energy gain experience a defocussing force, while those behind will experience a focussing force. A finite length beam of finite radius but with no transverse momentum (zero transverse phase space) entering the field region will leave with a spread in transverse momentum and a finite transverse phase space.

It is clear that if the rf fields did not vary during the time that any electrons were present in a cavity, there would be no phase dependent effects. The solution to the rf phase dependence problem which we are pursuing can be viewed as an attempt to approximate the ideal of no time dependence to the field seen by the electron bunch. Our approach is to include accelerating fields at harmonics of the fundamental frequency in the linac. For relativistic electrons in cylindrically symmetric fields the concept is clearly valid. In this case the energy gain of any electron is independent of radial position, and is strictly proportional to the cosine of its phase relative to the rf field. As this statement is true for any frequency field, frequencies at harmonics of the fundamental can be used to Fourier synthesize any desired effective time dependence of the energy gain. For example, a single frequency at the n^{th} harmonic can be used to 'flat-top' the dependence of the energy gain vs. rf phase by cancelling the second derivative of the fundamental at its peak.

The concept just described of using harmonic field to 'flat-top' the energy gain of a bunch of electrons also reduces the growth of transverse phase space. Maxwell's equations tell us that the magnetic fields, which are largely responsible for the transverse focussing forces, arise from the time rate of change of the local electric field. Thus, 'flat-topping' the electric field automatically minimizes the magnetic field, and the use of harmonics can simultaneously reduce longitudinal and transverse phase space growth.

For relativistic beams the compensating fields at the additional frequency (or frequencies) can be provided by cavities on the beam line which are

separate from the fundamental cavities. For non-relativistic beams the situation is substantially more complicated. An electron's energy gain is a function of radial position as well as relative phase, and the transverse force exerted on an electron is no longer linear in radial position. Since the radial and longitudinal motion of a non-relativistic electron within a cavity can be quite intricate, the harmonic fields should be superimposed on the fundamental field, and should have the same spatial dependence as the fundamental field so that the compensation can occur point by point. This ideal of point by point compensation is clearly impossible, as different frequency fields necessarily have different spatial distributions. Nonetheless, the concept of using a harmonic to reduce the time dependence of the net fields seen by the beam remains reasonable -- the caveat being that at low energies the various frequency fields must be as nearly superimposed as possible.

The validity of the harmonic compensation concept has been verified with the use of a version of the particle tracking code PARMELA⁵ modified to include the effects of rf fields at multiples of the fundamental. Figures 1 through 4 were generated by PARMELA, and are presented to illustrate the effect of the rf fields and space charge on the longitudinal and transverse phase space occupied by the beam. The rf fields used are those calculated by URMEL³ for a real cavity⁶ shaped to support accelerating fields at 1 GHz and at 3 GHz. The cavity length is 36 cm, including beam pipes.

All of the emittance figures to be presented refer to the area of an ellipse required to enclose 90% of the electrons in the distribution. The area quoted is obtained using a straightforward algorithm which gives a plausible estimate for the 90% area, but which is not in fact the absolute minimum area of an ellipse which could circumscribe 90% of the particles. As a result, the quoted emittance will be somewhat overstated, particularly for the highly disordered distributions which occur for high bunch charges. The algorithm actually used follows. First the average area for the distribution is calculated by associating with each particle the area of the ellipse defined by that particle. For this purpose the centroid of the ellipse is the same as that of the distribution, and the orientation of the ellipse and its aspect ratio, while arbitrary, is the same for each particle. The parameters describing the orientation and aspect ratio are then chosen to minimize the average area. Second, the ellipse associated with each particle using the parameters just determined is used to identify the particle whose ellipse encloses 90% of the distribution. Finally, the area of this particle's ellipse is used for the 90% emittance.

Figure 1 illustrates the advantages of multiple frequency acceleration, without the complications of space charge. A 1 cm diameter beam enters a single cell cavity and is accelerated from an initial energy of 1 MeV to about 2 MeV. The beam is 36 rf degrees long. Part (a) of the figure shows the output longitudinal and transverse phase spaces of the beam when the cavity is excited by only the fundamental frequency. The expected cosine dependence of the energy gain of individual electrons can be seen, as well as the rather typical 'butterfly' shape of the transverse phase space. Electrons at the back of the bunch occupy a narrow ellipse oriented from quadrant 2 to quadrant 4, while those at the front occupy a similar ellipse oriented from quadrant 1 to quadrant 3. Electrons at positions within the bunch occupy other ellipses such that the final distribution is as shown. Electrons in quadrants 2 and 4 will move closer to the axis as the bunch drifts

along the beam line, while those in quadrants 1 and 3 will move away from the axis. This illustrates the statement made earlier regarding the different focusing forces for particles at the front and back of the beam as a reason for growth in the transverse phase space of the beam. As seen on the figure, the transverse phase space has increased from $1 \pi \text{ mm mr}$, to $7.8 \pi \text{ mm mr}$, as a result of the rf dynamics associated with acceleration in a single cavity. Part (b) of the figure shows the results of exciting the cavity at the third harmonic in addition to the fundamental. The relative amplitudes and phases of the modes are adjusted as previously described to 'flat-top' the net energy gain versus phase of the electrons. As expected, the addition of the third harmonic results in an improvement of both the longitudinal and transverse phase space of the output beam. At the same time that the energy spread of the beam is reduced from 50 KeV to 1 KeV, the output transverse phase space has been reduced by a factor of four.

Figure 2 shows the results of three calculations chosen to demonstrate the importance of space charge and the advantage of reducing space charge forces by using a long beam bunch. The input beam for all three cases has an energy of 300 KeV, a bunch charge of 1 nC, a transverse phase space of $1 \pi \text{ mm mr}$, and a starting diameter of 1 cm. Part (a) of the figure shows the results of accelerating a beam which begins as a pulse ± 2 deg long through a single cell to an energy of about 1.2 MeV. Parts (b) and (c) show the results for a ± 6 and a ± 18 deg beam respectively. Acceleration is provided by fields at the fundamental for (a) and (b), and by fields at the fundamental and the third harmonic in (c). Note that the shape of the beam bunch ranges from a disk in (a) to a rod in (c). In order that the calculations be reasonable, and that comparisons among the three cases be meaningful, the cavity is preceded and followed by a thin solenoid lens. The first lens strength is chosen to let the beam drift to the center of the cavity with minimum transverse phase space growth with the cavity fields off. The second lens is adjusted for a minimum in angular spread at its exit. In comparing the three cases, it is clear that the long bunch suffers much less transverse space degradation than the short bunch. Actually, the degradation of the ± 18 deg case is even less than it appears, since the nearly vertical 'jets' visible in the distribution represent a rather small number of electrons at the ends of the bunch. Modest chopping of the beam would lead to a substantial increase in the beam brightness at a small peak current cost. Interpretation of the longitudinal phase space data is not so simple. While the calculated longitudinal phase space of the output beam is largest for the longest input beam, it is clear from the figure that there is a very high degree of correlation between energy and phase in the ± 18 deg case which is not taken into account by placing an ellipse around the distribution. In fact, the distribution bears a strong resemblance to a third order polynomial and leads to the speculation that if the amplitude and phase of the third harmonic field were adjusted properly, the phase ellipse would collapse substantially.

It is possible that unexpected results might appear after acceleration by several sequential 'flat-topped' cavities, even though the results after one cavity are very encouraging. The phase space occupied by the beam after the first, second and third cavities of the three cavity accelerator is displayed in parts (a), (b), and (c) of Figure 3. The rf fields in each cavity are 'flat-topped' with a third harmonic as discussed earlier. The energy gain in each cavity

is approximately 1 MeV. The input beam for the calculation has a kinetic energy of 300 KeV, a bunch length of ± 18 deg, a charge/bunch of 1 nC, a radius of 3 mm, and a normalized transverse phase space of 1π mm mr. A thin solenoid lens is placed immediately before the first cavity, and another between the first and second cavities. The strengths of the lenses are adjusted for minimum transverse phase space at the output of the first and third cavities. Examination of Figure 3 reveals nothing particularly surprising about the beam as it progresses through the sequence. The longitudinal phase space grows slightly from the beginning to the end, but in an orderly fashion, and probably by an amount significantly less than it appears. The transverse phase space actually seems to decrease somewhat from the exit of the first cavity to the exit of the last cavity! While the decrease is small, it is well within the accuracy of the calculation and presumably is obtained at the expense of some growth of the longitudinal phase space.

The final figure (Figure 4) of the series of beam calculations explores the possibility of using one cavity to produce the fundamental frequency field and another to produce the third harmonic field. As discussed earlier, there are reasons to believe that the separated cavity approach will be inferior to the single, multiple resonant cavity approach -- particularly for low energy beams. On the other hand, the engineering problems to be solved in order to use one cavity for the production of fields at more than one frequency are substantial. Immediate examples include tuning each frequency mode, coupling rf power to each mode, and sampling the modes independently for field and phase control. Production of each field in a separate cavity obviously solves all of these interaction problems at once. Figure 4 shows the evolution of a beam through a two cavity multiple frequency system. The first cavity is excited at the fundamental only, while the second cavity is excited at the third harmonic only. The input beam for the calculation has a kinetic energy of 300 KeV, a bunch length of ± 18 deg, a charge/bunch 1 nC, a radius of 4 mm, and a normalized transverse phase space of 1π mm mr. A thin solenoid lens is placed immediately before the first cavity, and another immediately after the second cavity. The strength of the first lens is adjusted for minimum transverse phase space at the output of the second cavity. The second lens is adjusted to minimize the angular spread at its output. From the figure it is clear that for this set of parameters, the separated cavity approach works quite well. The phase space of the beam after the first (fundamental only) cavity has been substantially degraded from the input. However, correlations within the beam are sufficiently well preserved during the 36 cm drift between cavities that the third harmonic field within the second cavity is able to reduce the beam phase space to a very respectable 7.6π mm mr by the time the beam leaves the cavity.

High Brightness Test Injector

Part of our program at Stanford includes the construction of a test injector incorporating the various concepts outlined in the preceding sections. Figure 5 is a block diagram of the injector along with some of its design parameters. The gun will operate at as high a dc voltage as practical. At present it is imagined that this limit is 300 or 400 kV. Whether the 333 ps pulses delivered by the block on the figure are obtained with a gridded gun in conjunction with an rf chopping system, or from

a photo-cathode remains to be seen. The harmonic buncher block incorporates multiple frequency fields to provide bunching with minimal phase space growth. The resulting ± 18 deg bunch will be accelerated to an energy of about 2.5 MeV by superconducting cavities providing fundamental and harmonic fields in separate cells. Finally the beam will be compressed with a magnetic bunching system by a factor of 10 or 20 to provide peak currents of a few hundred Amperes. The anticipated normalized transverse emittance of the beam is less than 20π mm mr, leading to a brightness in excess of 10^8 A/cm²/rad². The entire injector system will be carefully instrumented in order to properly study the phase space growth mechanisms.

Acknowledgements

The ideas presented here are from the group headed by Professor H. Alan Schwettman at the High Energy Physics Laboratory at Stanford University. Special thanks are due him and to Carl Hess of Stanford and to John Edighoffer of TRW. The computer code URMEL was provided by T. Weiland of DESY. The code PARMELA was provided by K. Crandall and L. Young of LANL.

References

1. Thomas C. Marshall, "Free Electron Lasers," (McMillan, Inc., New York, 1985) p. 23.
2. L. Elias and G. Ramian, "Status Report of the UCSB FEL Experiment Program," Free Electron Generators of Coherent Radiation, Charles A. Brau, Stephen F. Jacobs, Morton O. Scully, Editors, Proc. SPIE 453, pp. 140-145.
3. T. Weiland and J. Tuckmantel, "URMEL, Long Range Forces in the Frequency Domain," DESY Report M82-07, DESY Notkestrasse 85, 2000 Hamburg 52, FDR, (V. 2.06).
4. H. A. Schwettman, T. I. Smith, C. E. Hess, "Electron Acceleration Using High Gradient Single Cell Resonators," 1985 Particle Accelerator Conf. Vancouver, B.C., IEEE Trans. Nucl. Sci. NS-32 (1985).
5. K. Crandall and L. Young, "PARMELA: Particle Motion in Electron Linear Accelerators," Los Alamos National Laboratory (private comm.).
6. C. E. Hess, H. A. Schwettman, T. I. Smith, "Harmonically Resonant Cavities for High Brightness Beams," 1985 Particle Accelerator Conf., Vancouver, B.C., IEEE Trans. Nucl. Sci. NS-32 (1985).

Figure Captions

Figure 1: Phase space of an electron beam after being accelerated in a single cavity. The input beam is 1 cm in diameter. It is accelerated from an initial energy of 1 MeV to about 2 MeV. The input transverse phase space is 1π mm mr. The input bunch length is ± 18 rf degrees. For this figure, and the others presented, the units are cm, mr, keV, and degrees (1 GHz) for x, dx/dz, energy, and phase respectively. The plotted phase space distributions are an artist's rendition of the actual distribution which was calculated using 2000 particles. Each of the phase space projections which form the various spectra and profiles contain all 2000 particles.

(a) Phase space after acceleration by fundamental fields only,

(b) Phase space after acceleration by 'flat-topped' fields formed by the fundamental and the third harmonic. Note the improvement in the energy spectrum and the transverse phase space relative to (a).

Figure 2: Effect of bunch length on the output phase space of a bunch containing 1 nC. The input beam has an energy of 300 keV, a transverse phase space of 1π mm mr, and a diameter of 1 cm. Acceleration to approximately 1.2 MeV is provided by a single cavity. A lens before the cavity is adjusted for each case to minimize phase space growth to the center of the cavity with the cavity fields off. A lens after the cavity is adjusted to minimize the angular spread of the output beam.

(a) Input bunch length ± 2 deg (.33 cm). Acceleration by fundamental fields only.

(b) Input bunch length ± 6 deg (1.0 cm). Acceleration by fundamental fields only.

(c) Input bunch length ± 18 deg (3.0 cm). Acceleration by fundamental fields plus third harmonic fields.

Figure 3: Output phase space as a function of cavity number along a three cell accelerator. The fields in each cell are 'flat-topped' using the third harmonic, and provide approximately 1 MeV energy gain. The input beam has a kinetic energy of 300 keV, a bunch length of ± 18 deg, a charge/bunch of 1 nC, a radius of 3 mm, and a normalized transverse space of 1π mm mr. A thin solenoid lens is placed before the first cavity and another between the first and second cavities. The strengths of the lenses are adjusted for minimum transverse phase space at the output of the first and third cavities.

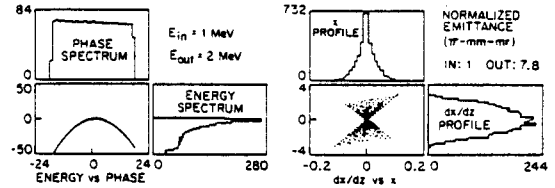
- (a) After the first cavity.
- (b) After the second cavity.
- (c) After the third cavity.

Figure 4: Output phase space of a beam accelerated from 300 keV to 1.1 MeV using a cavity with only fundamental fields followed by a cavity with only third harmonic fields. The input beam has a diameter of 8 mm, a charge/bunch of 1 nC, a pulse length of ± 18 deg, and a transverse phase space of 1π mm mr. A thin solenoid lens immediately in front of the first cavity is adjusted for minimum transverse phase space at the output of the second cavity. A thin lens at the output of the second cavity is adjusted for a narrow spread in angular divergence of the output beam.

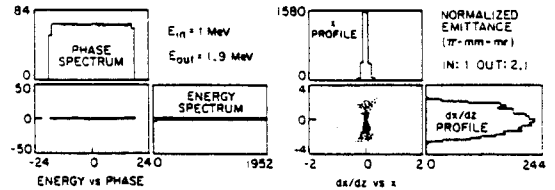
- (a) Phase space after the first cavity (fundamental only).
- (b) Phase space after the second cavity (third harmonic only). Note the improvement in phase space after the beam has passed through the second cavity.

Figure 5: Block diagram of the injector being constructed at the Stanford High Energy Physics Laboratory for the purpose of testing concept outlined in the text.

SINGLE CAVITY PHASE SPACE
Input Beam Diameter = 1 cm, No Space Charge



(a) FUNDAMENTAL ONLY

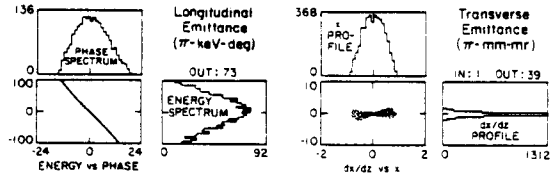


(b) FUNDAMENTAL PLUS THIRD HARMONIC

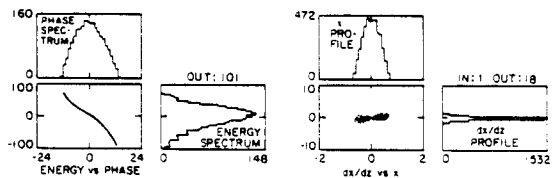
Figure 1

OUTPUT PHASE SPACE vs INPUT BUNCH LENGTH

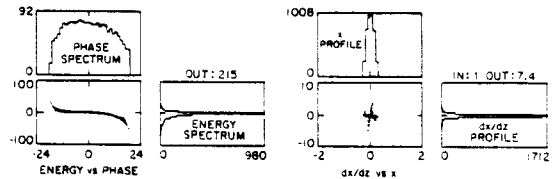
Bunch Charge = 1 nC
Input Diameter = 1 cm
Energy In = 300 keV
Energy Out \approx 1.2 MeV



(a) INPUT BUNCH LENGTH $\pm 2^\circ$, FUNDAMENTAL ONLY



(b) INPUT BUNCH LENGTH $\pm 6^\circ$, FUNDAMENTAL ONLY



(c) INPUT BUNCH LENGTH $\pm 18^\circ$, FUNDAMENTAL PLUS THIRD HARMONIC

Figure 2

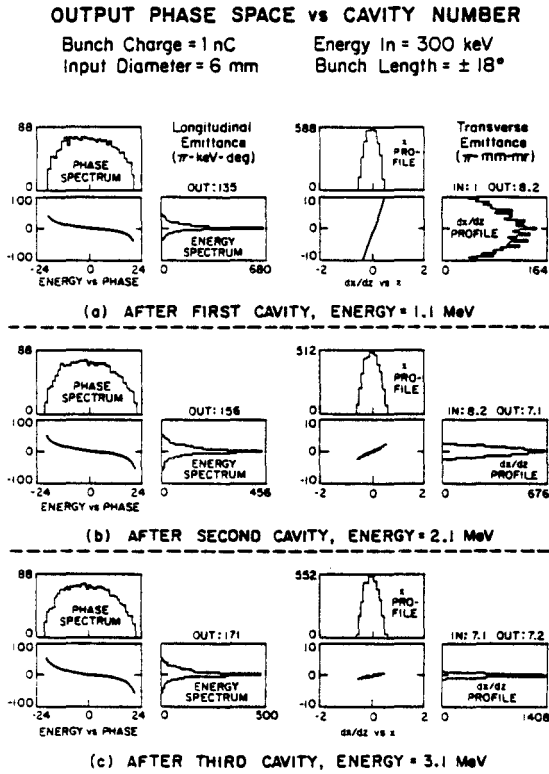


Figure 3

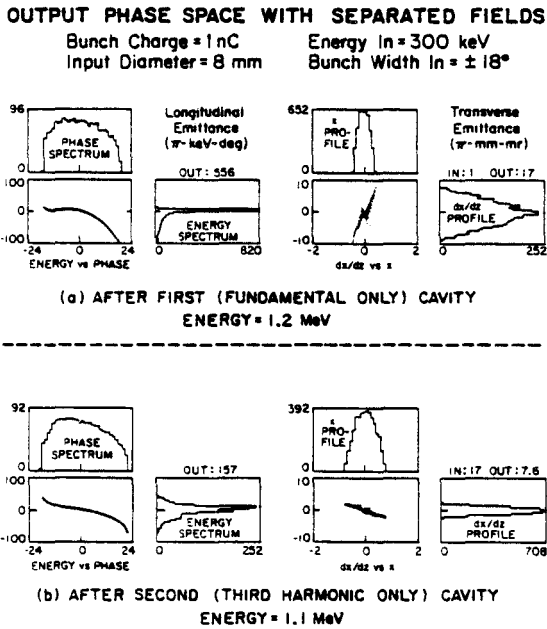


Figure 4

HIGH BRIGHTNESS INJECTOR

Injector Energy 2.5 MeV
 Average Current 10 mA
 Charge per Bunch 1.0 nC
 Transverse Emittance 20π mm-mr
 Peak Current 200 A
 Beam Brightness 10^8 A/cm²/rad²

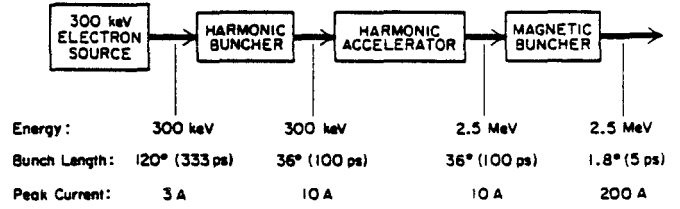


Figure 5